JJBS

Jordan Journal of Biological Sciences

Volume 12, Number 4,September 2019
ISSN 1995-6673
Pages 395 - 401

Photo-protective Measurements of Almond Oil on UVB-Irradiated Mouse's Skin and Cyclin D1 Expression

Azad K. Saeed*

Anatomy and Histopathology Department, College of Veterinary Medicine, Sulaimani University, KRG-Iraq

Received October 7, 2018; Revised November 16, 2018; Accepted November 25, 2018

Abstract

UVB radiations are among the major contributors for developing different skin lesions in humans and animals. This study was designed to show the photo-protective role of both natural and commercial almond oils against the skin lesions and cyclin D1 expression induced by UVB irradiations. A total of forty adult mice (six-weeks old), were employed in this study and distributed randomly to four groups (10 mice/group) as follows: Group A (control group, without UVB irradiation and treatment), Group B irradiated with UVB only, Group C (irradiated with UVB and treated with natural almond oil), and Group D (irradiated with UVB and treated with commercial almond oil). Histomorphometry was performed for each case by measuring skin layers' thickness, measuring the diameter of epidermal inclusion cysts and scoring the cyclin D1, and counting the positive cells. Group A, demonstrated the normal skin layers' thickness (Epidermis: 6.9±0.05µm, dermis: 64.1±2.16µm, hypodermis: 27±3.84µm). In group B, UVB increased the skin layers' thickness (Epidermis: 125.5±6.43µm, dermis: 148.2±7.84µm, hypodermis: 131.5±9.99µm) with a mean number 14 for epidermal inclusion cysts. Natural almond oil reduced the layers' thickness: 65.9±2.78µm (Epidermis), 98.4±6.98µm (Dermis), 112.4±7.46µm (Hypodermis), but the epidermal inclusion cysts were 15.6. While group D, the commercial almond oil was less photo-protective in comparison to the natural almond oil. Skin thickness became: 73.5±3.52µm (Epidermis), 107.5±7.73µm (Dermis), 114.4±4.33µm (Hypodermis) with increasing the epidermal inclusion cyst to 20.4. The counting system for cyclin D1 revealed 15.9±0.5, 37.9±0.45, 38.6±0.99, 36.6±1.36 for groups A-D respectively. Almond oil had a beneficial role in reducing skin thickness upon UVB irradiations, but it had the risk to develop epidermal inclusion cysts and no effective role in cyclin D1 expression.

Keywords: Almond oil, Cyclin D1, Epidermal inclusion cyst, Skin thickness, UVB.

1. Introduction

Sun rays reaching to the surface of the earth are classified into three different types of radiations. UV light (200-400nm), visible light (400-700nm), and infrared radiations (760-5100nm). UV radiations, especially under 320nm, play a significant role in most of the deleterious effects on the skin depending on length and frequency of exposure. Both UVA and UVB radiations can cause sunburns, photo aging, pigmentation, skin cancers, and various painful effects. Hence, there is a need for agents reported to have UV shielding effect. Generally, sunscreens are used to protect skin from the damaging effects of sun rays (Webber *et al.*, 1997; Bair *et al.*, 2002; Saeed, 2011; Saeed and Salmo, 2012; Kulkarni *et al.*, 2014).

There is a confirmation by skin care agencies that commercial sun blockers have a quick sun-protective action, but may have negative effects at the same time. It is beneficial to use herbal ingredients as they do not trigger allergic reactions, comedogenic effects, and any other side effects (Mishra *et al.*, 2011). Therefore, many plant components are extensively incorporated in the formulation because of their properties such as their strong effects, safety, purity, stability in cost, availability in different plants (Mishra *et al.*, 2011). Traditionally, almond oil has been used to keep the elasticity of the skin and youthful appearance, because its lipophilic ability in reducing the UV degradation of retinyl palmitate to the less active cis-isomers (Scalzo *et al.*, 2004, Sultana *et al.*, 2007).

Cyclin D consists of three different isoforms D1, D2, and D3. It plays a pivotal role in regulating cell cycle progression in the G1/S phase transition, and seems to be triggered by external growth stimuli rather than internal controls of the cell cycle. Cyclin D1 is the well-known example of D-type cyclin, which is related to cell cycle control and oncogenesis. Cyclin D1 is considered an important proto-oncogene because the overexpression of cyclin D1 leads to the reduction of the G1 phase and to less dependency on exogenous mitogens, producing abnormal cell proliferation which may lead to the inducing of addition genetic lesions (Guan *et al.*, 2018). The current study was designed to investigate the photo-protective role of both natural and commercial almond oils in reducing skin lesions and cyclin D1 expression induced by UVB exposure.

* Corresponding author e-mail: azad.saeed@univsul.edu.iq.

2. Materials and Methods

2.1. Animal Model

A total of forty adult albino mice (*Mus musculus* species, *BALB/c* strain, 20 males and 20 females), that are six-weeks old, at weights ranging 25-35g, were used in this experiment. After one week of acclimation, they were divided into four groups: Group A (n=10), which was the control group without UVB irradiation and treatment by almond oils. Group B (n=10) was irradiated with UVB light only. Group C (n=10) was irradiated with UVB and treated with natural almond oil. The remainder group (group D, n=10) was irradiated with UVB and treated with commercial almond oil. Mice were fed with a standard pellet diet (Pico Lab) and were provided with water *ad libitum*. They were housed in the animal house/ College of Veterinary Medicine/Sulaimani University, maintained at a controlled room temperature of about 25℃ and photoperiodicity of a twelve-hour light/dark system. The use of animals in the present study was in accordance with the review and institutional guidelines of the Ethic Committee (No. 14/2018) of the College of Veterinary Medicine/Sulaimani University.

2.2. UVB Irradiation

The mice were irradiated using a lamp of 312nm wavelength, and 15 watts (Vilber-Lourmat-France). The animals in groups B-D were exposed to UVB light for 30 minutes/day (5 days/week for 6 consecutive weeks) with a constant dose of 80mj/Sec throughout the experiments. An electric clipper was used to remove the dorsal hair for the sake of making a rectangular area (2x5 cm) prior to the UVB irradiation. During the period of irradiation, the mice could move around freely in a specially designed ventilated glass metal-free cabinet (30x25x25 cm).

2.3. Treatment of Mice with Almond Oils

The two types of natural and commercial almond oils were used in this experiment. The natural almond oil was extracted by an oil press. From each 250g of sweet almond, 50ml of oil was achieved. Commercial almond oil (Sweet Almond Oil 250 mL, Latin Name: *Prunus dulcis*) was purchased from Naissance Company-Swansea-UK. Mice from the groups C and D were treated with natural and commercial oils respectively for 5 days/week. The oil treatments were performed at two different times 15 minutes before exposure to UVB (5 drops=250µL) and after the UVB exposure directly (5 drops=250µL).

Gallic acid, Catching, Epicatechin, Caffeic acid, Vanellic acid, Cinnamic acid, and vitamins A and E) were detected from the imported and lab-extracted oil using High Performance Liquid Chromatography ultraviolet (HPLC-UV). All the samples of almond oils were extracted by the solid phase extraction (SPE) method in the lab for the main compounds, were injected in HPLC in the Ministry of Science and Technology lab (Baghdad), and were separated under the optimum conditions.

The results show that the imported samples contained 0.0367 µg/L of vitamin A and 0.0413 µg/L of vitamin E, while the lab extracted samples contained 0.0312 µg/L of vitamin A and 0.06018 µg/L of vitamin E. Moreover, the Gallic acid, Catechin, Epicatechin, Caffeic acid, Vanellic acid, and Cinnamic acid showed no peaks.

2.4. Skin Biopsy Collection

At the end of the experiment, the mice were sacrificed by cervical dislocation as humane euthanasia. The samples were taken from the dorsal skin, fixed immediately in 10% neutral buffered formalin for 24 to 48 hours, and were routinely processed in the histopathology lab of the teaching hospital and Shorsh hospital/Sulaimani Governorate. The samples were embedded in paraffin blocks after which two sections from each sample were taken at a 5µm thickness for Hematoxylin and Eosin (H&E) staining. The second section was put on a positively-charged slide proceeding with the process of immunohistochemistry staining following the manufacturers' instructions provided with the kit of anti-Cyclin D1 (Monoclonal rabbit anti-human, Cyclin D1, Clone EP12, Dako, Denmark).

2.5. Quantitative Assessment

The slide sections of the dorsal skin were checked out under light microscope (Leica Motic); equipped with an image analysis system (ToupTek, ToupView, x64, 3.7.4183, 2014, linked to a computer) at the Anatomy and Histopathology Department/College of Veterinary Medicine/Sulaimani University. In each case, the full skin thickness was recorded in five randomly selected fields, including epidermal, dermal and hypodermal thickness independently at 100-fold magnification (x100), and then the mean was calculated for each sample. For the quantification of the epidermal inclusion cysts which were formed in the groups B-D, the number of cysts was counted throughout the slides, and then the numbers were calculated to obtain the mean of the group. For each cyst, the diameter was recorded through four cross lines, then at a cross point. The diameter was calculated as mentioned elsewhere (Park and Ko, 2013). The measurements were reported in micrometer values (Figure 1).

2.6. Cyclin D1 Scoring

The positive cells in the epidermal keratinocytes of five sections with highly expressed cyclin D1 were counted at high-power magnification (x400) for each specimen, then the mean values were obtained, and finally a comparison was carried out for different groups.

A score system was designed according to the location of positive cells, which included: score 0, for negative staining, score 1+ (positive cells were restricted to stratum basale and stratum spinosum), score 2+ (positive cells in all layers of epidermis), and score 3+ for positive cells in epidermal layers and follicular epithelial cells).

2.7. Statistical Analysis

For the comparison among different groups, the mean ± SEM were determined. Both one-way ANOVA Tuckey test and Pearson's correlation coefficients were performed using the SPSS software, version 16; a P value of <0.05 was considered statistically significant.

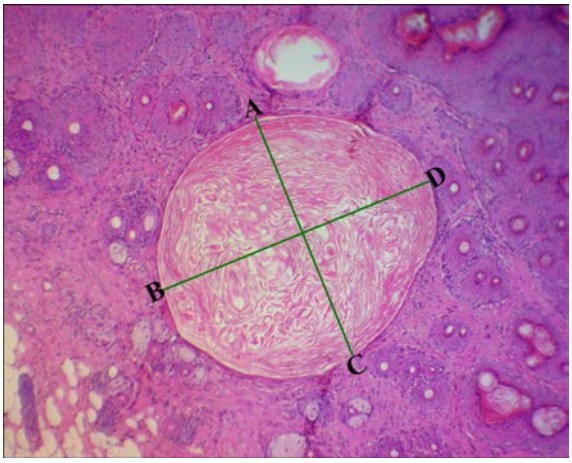

Figure 1. Epidermal inclusion cyst's diameter (µm) was recorded at the averaged value between AC and BD line (H&E stain, x100).

3. Results

No differences in the response to almond oils were recorded between males and females. In the following sections, differences in the skin histology as well as levels of expression of cyclin D1 after different treatments were described in some details.

3.1. Control

The mice from group A, showed normal features of skin which grossly appeared as a thin and delicate layer (Figure 2a). Microscopically, all the components of mouse skin were thoroughly examined, including:

Epidermis: The outermost part of the skin composed of three-four sub-layers. The stratum basale and stratum spinosum were prominent, while the stratum granulosum had been often unapparent, it appeared as the intermittent layer, keratohyalin granules were seen in some individual cells. The thickness of the stratum corneum was variable; for instance keratin materials in some sections were detached while in the others a thin layer persisted. The epidermis in the control group was the thin layer which was about 6.9±0.05µm (Table 1), and made up 7% of the whole skin thickness (Figure 2b-c, 3).

Dermis: The second layer located under the epidermis, which was composed of densely packed, randomly oriented, thick bundles of collagen. Most of the skin appendages, with the exception of sweat gland, were found in this layer including pilosebaceous apparatus (Hair follicles, sebaceous glands, and arrector pili muscles). It was the thickest layer of the skin, which was 64.1±2.16µm (Table 1) constituting 65.5% of the total skin thickness (Figure 2b-c, 3).

Hypodermis (Subcutis): The inner layer of the skin, which was highly variable in appearance. It is composed of an adipose connective tissue, collagen fibers with associated blood vessels, nerve fibers, and hair follicles. The thickness of the hypodermis layer was about 27±3.84µm (Table 1) and approximately made up 27.5% of the total skin thickness (Figure 2d, 3).

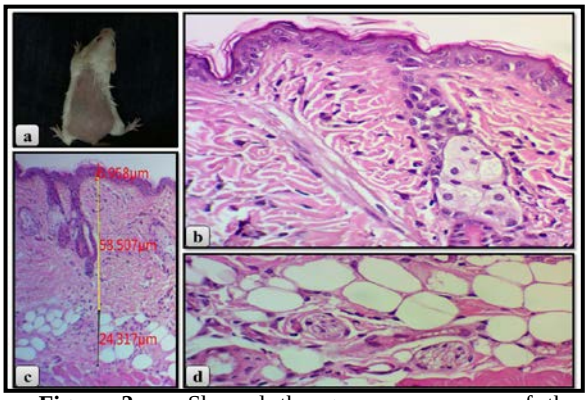

Figure 2. **a**: Showed the gross appearance of the normal mouse skin in the dorsal rectangular shaved area. **b**: Histologic view of the mouse skin, a thin epidermal layer was observed with the dermal view which contained pilosebaceous unit with large numbers of collagen fibers (H&E stain, x400). **c**: Measurement values for skin sublayers epidermis (red line), dermis (yellow line) and hypodermis as indicated by black line (H&E stain, x100). **d**: Hypodermis was composed of loose connective tissue, adipocytes with associated blood vessels, and nerve fibers (H&E stain, x400).

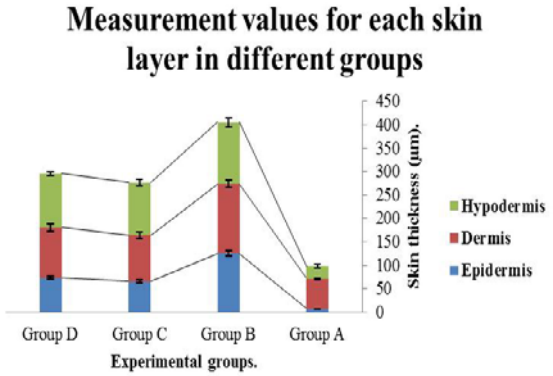

Figure 3. Averaged thickness (µm) of the skin layers (epidermis, dermis, and hypodermis) measurements recorded by histology were separated into different groups. Variation in the thickness of the skin sublayers was the most significant difference among the groups. Group A was regarded as a standard for comparison to the other groups, the most significant thickness was observed in group B in which it increased by 4-fold while in group C and D it declined to 3-fold. Error bars correspond to the standard error of the mean.

3.2. UVB Irradiation

Dorsal skin gross inspection of the mice in this group revealed variable lesions including increased skin thickness detected by many skin wrinkles and hand palpations, focal patches of alopecia with small ulcers (Figure 4a).

Microscopical examination: Chronic UVB irradiation induced multiple lesions from the epidermis to the hypodermis. But most of them were localized to the epidermis such as the increase of the epidermal thickness to 125.5±6.43µm as a result of the proliferating effect of UVB, which increased the skin thickness by 18.1 fold in comparison to the control group ($r_{pearson}$=0.922, p=.000), which constituted 31% of the total skin thickness (Figure 3, Table 2). The difference in epidermal thickness of the skin between the control mice (group A) and UVB- treated mice (group B) was statistically significant. Furthermore,

different lesions were found in the epidermis including sunburn cells, vacuolization, intercellular edema, dyskeratosis with acantholysis (Figure 4b-e)

The dermal lesions included increasing dermal thickness to 148.2±7.84µm which was 2.3 times more than the normal dermal thickness ($r_{pearson}$=-0.931, p=.000), making up 36.5% of the total skin thickness in group B (Table 2, Figure 3 and 5a), as well as hyperplasia of the sebaceous glands, and loss of hair follicles with the evidence of perifolliculitis (Figure 5b-c). The most prominent lesion in this layer was the formations of a large number of epidermoid inclusion cysts with variable sizes (ranging from 10 to 75 μm^2) and variable forms (Capsulated and inflamed) as a result of degeneration in the hair follicles with associated sebaceous glands. Moreover, the dermis was filled with inflammatory cells and implanted keratinocytes; the latter participated in the formation of the capsule of epidermal inclusion cysts. Histologically, the capsulated cysts were composed of concentrically laminated keratin surrounded by stratified squamous epithelium or a thin layer of fibrosis. Whereas the inflamed cysts were composed of keratin materials with a mixture of inflammatory cells, degenerative cells of hair follicles, and sebaceous glands with implanted keratinocytes (Figure 5d-e, 6a-b).

Pathological lesions in the hypodermis included increased thickness to 131.5±9.99µm which was 4.8 times more than in the control group ($r_{pearson}$=-0.708, p=.000) contributing to 32.5% of the whole thickness (Figure 3, 7a). This indicates that there was a significant correlation between UVB exposure and hypodermal thickness. In addition, the hypodermis showed less frequent epidermal inclusion cysts in comparison to the dermis, fat necrosis with infiltration of mononuclear inflammatory cells with few multinucleated giant cells (Figure 7b-c). The estimated mean number of the epidermal inclusion cysts in this group was 14.

Table 1. Epidermal, dermal, and hypodermal thickness values (µm) for different cases among different groups:

	Group A (Control group)			Group B (Exposure group)			Group C (Natural oil)			Group D (Commercial oil)		
	Epidermis	Dermis	Hypodermis	Epidermis	Dermis	Hypodermis	Epidermis	Dermis	Hypodermis	Epidermis	Dermis	Hypodermis
1.	6.6	52.2	17.7	155	175.2	195.3	46.6	67.6	84.9	53.1	65.3	106.3
2.	6.6	58.2	19.1	146.1	174.1	159.9	60.2	77.4	92.4	62.2	84.3	90.9
3.	6.8	61.3	19.2	140.3	170.1	154.6	61.3	83.9	97.5	89.8	93.3	125.9
4.	6.9	61.9	21.6	134.9	169.8	147.9	62.4	84.8	104.1	87.4	97.1	91.8
5.	6.9	62.1	22.1	126.1	159.5	126.1	67.6	93.4	108.2	76.6	105.9	117.7
6.	6.9	63.3	22.2	122.2	144.4	112.6	68.4	102.9	109.9	73.3	113.4	117.9
7.	7	66.6	24.9	122.3	129.7	109	69.6	107.7	113.4	75.5	116.5	128.5
8.	7.1	69.6	30.3	121.9	129.6	108.5	70.9	110.1	120.3	66.9	122.2	126.8
9.	7.2	70.2	43.5	95.1	123.7	104.2	75.6	111.7	123.4	80.5	123.2	116.5
10.	7.3	76.5	49.8	91.3	106.3	97.5	76.7	144.9	170.3	70.1	154.3	122.2
Mean±SEM[a]	6.9±0.05	64.1±2.16	27±3.84	125.5±6.43	148.2±7.84	131.5±9.99	65.9±2.78	98.4±6.98	112.4±7.46	73.5±3.52	107.5±7.73	114.4±4.33

[a]: Standard error of the mean

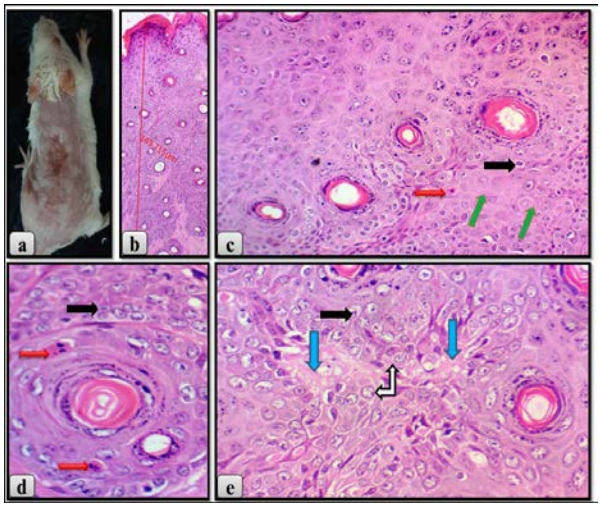

Figure 4. **a**: An ulcer with an increasing skin thickness at the boundaries and loss of hair in some regions. **b**: Diffuse keratinocytes proliferation which led to increasing epidermal thickness (H&E stain, x100). **c-e**: There were multiple lesions in the epidermal cells, including apoptotic cells (Red arrows), vacuolated cells (Black arrows), intercellular edema (Blue arrows), dyskeratotic cells (Green arrows) with acantholytic cells as marked by left–up white arrow (H&E stain, x400).

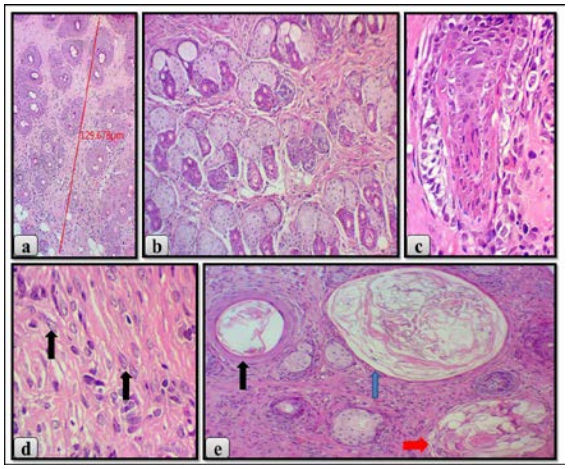

Figure 5. **a**: Dermal thickness value measurement (H&E stain, x100), **b**: Hyperplasia of the sebaceous gland with associated hair follicles (H&E stain, x100), **c**: Perifolliculitis as a pattern of hair follicle inflammation arising from the degenerative effect of UVB on the hair follicle (H&E stain, x400), **d**: Invasion of the large numbers of epidermal keratinocytes into the dermis (Black arrows) which participated in the formation of capsules of epidermal inclusion cysts (H&E stain, x400). **e**: Different forms with variable sizes of epidermal inclusion cyst such as cysts surrounded by stratified squamous epithelium (Black arrows), the blue arrow indicates a cyst lined by a thin layer of fibrous tissue, and the red arrow demonstrates an inflamed type of cyst surrounded by a mixture of degenerated cells from hair follicles and sebaceous glands, inflammatory cells and implanted keratinocytes (H&E stain,x100).

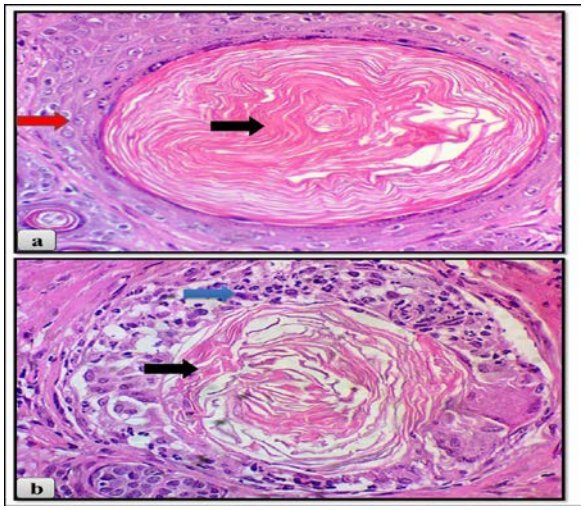

Figure 6. Microscopic features of an epidermal inclusion cyst, **a**: Stratified squamous epithelium with inner granular layer (Red arrow) surrounded by a laminated keratin (Black arrow), **b**: Inflamed type keratin materials (Black arrow) surrounded by degenerative cells of the hair follicle and sebaceous cyst, inflammatory cells and keratinocytes (Blue arrow, H&E stain, x400).

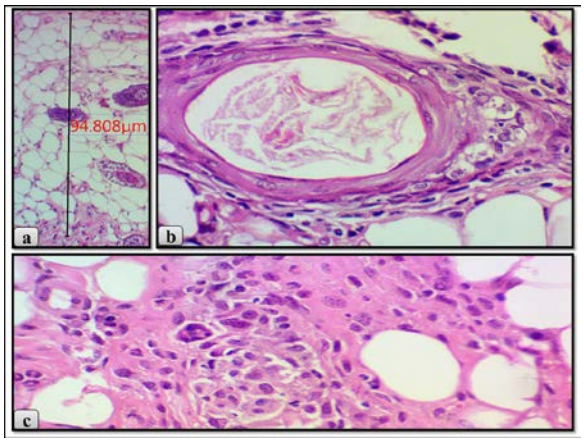

Figure 7. Microscopic features of hypodermis in group B, **a**: Thickness value measurement for hypodermis (Black line, H&E stain, x100), **b**: Degeneration of the hair follicle and formation of epidermal inclusion cyst (H&E stain, x400), c: UVB-induced panniculitis characterized by the presence of necrotic adipocytes, inflammatory cells with few multinucleated giant cells.

3.3. UVB plus Natural Almond Oil

Mice from the group of UVB-natural almond oil showed all of the lesions of group B but in a milder form. The light microscopy revealed that the UVB exposure induced epidermal hyperplasia with epidermal thickness to 65.9±2.78µm ($r_{pearson}$= 0.921, *p*=.000) making up 23.8% of the total skin thickness (Figure 3), which was 8.6 times less severe than the exposure group ($r_{pearson}$=-0.923, *p*=.000). This indicated that natural almond oil had a positive effect against the increasing skin thickness induced by UVB. Many lesions were found in the epidermis including apoptosis, vacuolation of keratinocyte, dyskeratosis with acantholytic changes (Figure 4). In the dermis, the dermal thickness descended to 98.4±6.98µm which made up 35.5% of the whole skin thickness ($r_{pearson}$=0.965, *p*=.000), although the numbers of epidermal inclusion cysts increased in both dermis and hypodermis with the mean number of 15.6. The majorities of these cysts were of the inflamed types, sebaceous hyperplasia, and some of them started to degenerate with associated hair follicles and the existence of implanted epithelial cells and inflammatory cells. In hypodermis, most of the lesions persisted; the hypodermal thickness was reduced to 112.4±7.46µm which was 0.85 times less than in the exposure group ($r_{pearson}$=-0.775, *p*=.216) and 4.1 times more than the control group ($r_{pearson}$=0.912, *p*=.000) making up 40.7% the total skin thickness (Figure 3). Fat necrosis, inflammatory cells, degeneration of the distal parts of the hair follicles with a number of epidermal inclusion cysts were seen in this region.

3.4. UVB plus Commercial Almond Oil

Grossly, all the above lesions were recognized without obvious differences. The microscopical examination indicated that the lesions in this group were more pronounced than in group C and less severe than in the group B. The epidermal thickness was 73.5±3.52µm (25% of the skin thickness), 7.5 times reduced the hyperplastic effect of UVB ($r_{pearson}$=0.968, *p*=.000), and 10.6 times thicker than the control group ($r_{pearson}$=-0.960, *p*=.000). The dermal thickness decreased to 107.5±7.73µm (36% of the skin thickness), in comparison to 0.7 times less than the exposed group ($r_{pearson}$=-0.934, *p*=.001), and 1.6 times more than the control group ($r_{pearson}$=0.981, *p*=.000). The epidermal inclusion cyst counting recorded the highest number in this group with a mean number of 20.4. In hypodermis, the thickness was 114.4±4.33µm (39% of the total skin thickness), which was 4.2 times more than the control group ($r_{pearson}$=0.356, *p*=.000), 0.6 times less than exposed group ($r_{pearson}$=-0.589, *p*=.305).

Table 2. Increases in the thickness (µm) of the skin layers in the experimental groups relative to the control group.

Skin layers	Group A	Group B	Group C	Group D	Group B Vs. group C	Group B Vs. group D
Epidermis	1	18.1	9.5	10.6	8.6	7.5
Dermis	1	2.3	1.5	1.6	0.8	0.7
Hypodermis	1	4.8	4.1	4.2	0.7	0.6

3.5. Cyclin D1 Expression

The positive cells of cyclin D1 expressions appeared as the brown-stained nuclei showing extreme variability in intensity, numbers, and the location of the positive cells. The counted positive cells were listed in table 3 for each case in different groups. In the control group (Group A), the percentage of positive cells was 15.9% with score 1+. This indicated that the cells were scattered in both layers of stratum basale and stratum spinosum (Figure 8a), while in group B, the percentage of positive cells increased to 37.9% and the score changed to 3+ ($r_{pearson}$=-0.959, *p*=.000). This meant that UVB irradiations upregulated cyclin D1, increased the number of cells, and changed in the location of cells despite the presence in the stratum basale and spinosum. The positive cells extended upwards (toward the stratum granulosum "prickle layer") either as individual cells or clusters of cells. In addition to the presence of cyclin D1 in the epidermal kerationcytes, they were found in the follicular cells and the capsules of epidermal inclusion cysts (Figure 8b-e).

The average counts in the treatment groups (C and D) were not significantly different compared with group B, which were composed of 38.6% (Group C, *p*=.943) and

36.6% (Group D, *p*=.630) with the score 3+ for both groups.

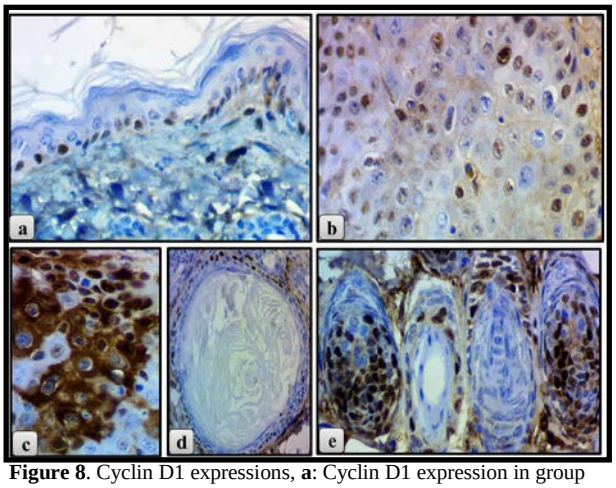

Figure 8. Cyclin D1 expressions, **a**: Cyclin D1 expression in group A (control), Score 1+: most of the cells were located in the stratum basale and stratum spinosum (x400), **b**: Score 3+; positive cells were scattered in all epidermal layers (x400), **c**: Small clusters of positive cells in the stratum granulosum (x400), **d-e**: Positive cells were found in the capsule of epidermal inclusion cyst and in the hair follicles (x100 and x400).

Table 3. Results of positive cells counting for cyclin D1 expression in different groups.

Case No.	Group A	Group B	Group C	Group D
1.	17	39	36	31
2.	18	37	43	32
3.	18	39	38	43
4.	15	37	35	38
5.	15	37	44	36
6.	13	38	41	36
7.	16	35	36	41
8.	17	38	38	35
9.	15	39	39	32
10.	15	40	36	40
Mean±SEM	15.9±0.5	37.9±0.45	38.6±0.99	36.6±1.36

4. Discussion

Ultraviolet radiation (UVR) can impair the integrity of skin barriers as the exogenous factor. Measuring mechanical and structural properties of skin is a complicated process involving thickness, elasticity, and variations associated with age and body sites (Wang *et al.*, 2013). Since the skin is composed of different layers of varying depths with different physical and chemical properties, UVR induces variable pathological lesions on different types of cells in the skin (Lee *et al.*, 2013). The current study revealed that the major changes occurred in the epidermis of animals exposed to UVB radiation. These findings were partly shown in previous studies by the same author such as the aforementioned correlations between UVB and epidermal thickness (Hassan *et al.*, 2015a, Hassan *et al.*, 2015b, Saeed *et al.*, 2016).

The effects of UVB radiation on the dermis and hypodermis are somehow not studied at all, despite the fact that UVB provokes the inflammatory reactions through indirect damage and leads to dermal elastosis as a result of chronic irradiations (Zhang and Zhu, 2012). The present work was aimed at illuminating the relationship among UVB, dermal, and hypodermal thickness. It revealed that UVB increased the dermal thickness by 2.3 fold while the hypodermal thickness increased by about 4.8 fold (*p*=.000).

Epidermoid inclusion cysts are the most frequent lesions with very little known etiology. They are mostly are formed as a result of degenerative changes in the pilosebaceous apparatus or invasion of epidermal keratinocytes into the dermis. Many factors can contribute to the occurrence of these cysts, including ruptured pilosebaceous follicle, progressive ductal defect, ductal obstruction of a sebaceous gland, or injurious implantation of surface epithelium under the skin (Zuber, 2002). Many references have mentioned the role of exogenous factors such as human Papillomavirus and UV in the induction of epidermoid cysts (Zeigler *et al.*, 1996, Lee *et al.*, 2003, Ramagosa *et al.*, 2008, Narain *et al.*, 2012, Sato *et al.*, 2014). Up to the author's knowledge, no previous studies have mentioned the role of UVB in the induction of epidermoid cysts in the back skin of mice, therefore, the current study could be considered as the first trial in this aspect.

In the past, almond oil was used as a complementary medicine by civilians of Greece, India, and China to treat different conditions, including skin lesions (psoriasis and eczema), problems of the cardiovascular and digestive system. Nowadays, it is commonly used in cosmetics industries because of its abilities in penetrating, moisturizing, and restructuring the skin (Ahmad, 2010). Many authors have investigated that some plant oils contain natural sunscreens. For instance, 30% of UV rays are blocked by sesame oil, whereas cottonseed, coconut, olive, and peanuts oils can block out about 20% of UV rays (Anitha, 2012). Presumably, no previous studies have reported the role of almond oil as a natural sunscreen. On the basis of this investigation, it was observed that almond oils had a protective role in reducing skin thickness induced by UVB exposure. It was found that the natural almond oil reduced 48% of epidermal thickness, 34% of dermal thickness, and 15% of hypodermal thickness, whereas the commercial almond oil decreased 41% of epidermal thickness, 27% of dermal thickness, and 13% of hypodermal thickness (p=.000). These finding revealed that almond oils could be regarded as a substitution for commercial sunscreens. In a previous study by the same author, it was found that the application of sunscreens resulted in a 46% reduction in the epidermal thickness using the same animal model and duration period (Saeed *et al.*, 2016).

In contrast, almond oils may have negative effects leading to increasing the number of epidermal inclusion cysts in both groups (C and D) by 11% and 45% respectively. These changes have not been studied previously and they might be associated with blocking the pores of the pilosebaceous apparatus by the oils.

UV irradiations act on signaling pathways that affect the expression of cyclin D1 (Liu *et al.*, 2011). Previous evidences revealed that cyclin D1 overexpression is associated with skin tumor development and showed a positive correlation between the onset of cyclin D1 accumulation and the sudden increase in the number of tumors per animal (Kim *et al.*, 2002). In the present study, the same result was obtained and stated that chronic UVB irradiations increased the number of positive cells (by 2

fold) when compared to the positive cells of the control group. Additionally, the current study records, for the first time, the link between cyclin D1 expression and UVB irradiations, which is a new subject and, therefore, further studies are needed to explore more details on this basis.

5. Conclusion

UVB increases the thickness of all skin sublayers such as epidermis, dermis, and hypodermis with the incidence of epidermal inclusion cysts through epidermal invasion into the dermis and the degeneration of the pilosebaceous apparatus. Almond oils play a dual role in the mouse skin. Positively, it reduces skin thickness induced by UVB irradiations. Negatively, it increases the formation of epidermal inclusion cysts and seems to have no obvious role in reducing cyclin D1 expression. Further studies are necessary to demonstrate the biological role of cyclin D1 in the development of different skin lesions induced by UVB exposure.

Conflict of Interest

The author declares that there is no conflict of interest.

Financial Source

None

References

Ahmad Z. 2010. The uses and properties of almond oil. *Complement Ther Clin Pract.,* **16 (1)**: 10-12.

Anitha T. 2012. Medicinal plants used in skin protection. *Asian J Pharm Clin Res.,* **5 (3)**: 35-38.

Bair WB, Hart N, Einspahr J, Liu G, Dong Z, Alberts D and Bowden GT. 2002. Inhibitory effects of sodium salicylate and acetylsalicylic acid on UVB-induced mouse skin carcinogenesis. *Cancer Epidemiol Biomarkers Prev.,* **11 (12)**: 1645-1652.

Guan G, Bakr MM, Firth N and Love RM. 2018. Expression of cyclin D1 correlates with p27kip1 and regulates the degree of oral dysplasia and squamous cell carcinoma differentiation. *Oral Surg Oral Med Oral Pathol Oral Radiol.,* **126 (2)**:174-183.

Hassan SMA, Hussein AJ and Saeed AK. (2015a). Role of green tea in reducing epidermal thickness upon ultraviolet light-B injury in BALB/c mice. *Advances in Biology,* **2015**: 1-6.

Hassan SMA, Saeed AK and Mehdi AH. (2015b). Histopathologic effect of xylene and ultraviolet type B exposure on mouse skin. *Int J Curr Microbiol App Sci.,* **4 (5)**: 997-1004.

Kim AL, Athar M, Bickers DR and Gautier J. 2002. Stage-specific alterations of cyclin expression during UVB-induced murine skin tumor development. *Photochem Photobiol.,* **75 (1)**: 58-67.

Kulkarni SS, Bhalke RD, Pande VV and Kendre PN. 2014. Herbal plants in photo protection and sun screening action: An overview. *Indo Am j Pharm.,* **4 (2)**: 1104-1113.

Lee CH, Wu SB, Hong CH, Yu HS and Wei YH. 2013. Molecular mechanisms of UV-induced apoptosis and its effects on skin residential cells: The implication in UV-based phototherapy. *Int J Mol Sci.,* **14 (3)**: 6414-6435.

Lee S, Lee W, Chung S, Kim D, Sohn M, Kim M, Kim J, Bae H and Kam S. 2003. Detection of human papillomavirus 60 in epidermal cysts of nonpalmoplantar location. *Am J Dermatopathol.,* **25 (3)**: 243-247.

Liu S, Gonzalez J, Hwang BJ and Steinberg ML. 2011. Induction of cyclin d1 by arsenite and UVB-irradiation in human keratinocytes. *J Health Care Poor Underserved.,* **22 (4)**: 110-121.

Mishra AK, Mishra A and Chattopadhyay P. 2011. Herbal cosmeceuticals for photoprotection from ultraviolet B radiation: A review. *Trop J Pharm Res.,* **10 (3)**: 351-360.

Narain S, Gulati A, Yadav R and Batra H. 2012. Epidermoid cysts of face: Clinicopathological presentation and a report of four cases. *Int Clinic Dent Sci.,* **3 (1)**: 30-34.

Park JS and Ko DK. 2013. A histopathologic study of epidermoid cysts in korea: Comparison between ruptured and unruptured epidermal cyst. *Int J Clin Exp Pathol.,* **6 (2)**: 242-248.

Ramagosa R, de Villiers EM, Fitzpatrick JE and Dellavalle RP. 2008. Human papillomavirus infection and ultraviolet light exposure as epidermoid inclusion cyst risk factors in a patient with epidermodysplasia verruciformis. *J Am Acad Dermatol.,* **58 (5)**: S68.e1-S68.e6.

Saeed AK. 2011. EGFR protein expression after UVB radiation of mouse skin utilizing IHC technique, evaluation of total antioxidant status and assessing affectivity of antioxidants on EGFR expression. MSc dissertation, University of Sulaimani, Sulaymanyah, Iraq.

Saeed AK, Hassan SMA and Maaruf NA. 2016. Ultraviolet type B-radiation-induced hyperplasia and seborrheic keratosis is reduced by application of commercial sunscreens. *Pak Vet J.,* **36 (4)**: 450-454.

Saeed AK and Salmo N. 2012. Epidermal growth factor receptor expression in mice skin upon ultraviolet B exposure-seborrheic keratosis as a coincidental and unique finding. *Adv Biomed Res.,* **1**: 59.

Sato Y, Nozaki T, Matsusako M, Eto H, Matsui M, Ohtake N, Suzuki K, Starkey J and Saida Y. 2014. Human papillomavirus-associated plantar epidermoid cysts: MR and US imaging appearance. *Skeletal Radiol.,* **43 (2)**: 257-261.

Scalzo M, Santucci E, Cerreto F and Carafa M. 2004. Model lipophilic formulations of retinyl palmitate: Influence of conservative agents on light-induced degradation. *J Pharm Biomed Anal.,* **34 (5)**: 921-931.

Sultana Y, Kohli K, Athar M, Khar R and Aqil M. 2007. Effect of pre-treatment of almond oil on ultraviolet B–induced cutaneous photoaging in mice. *J Cosmet Dermatol.,* **6 (1)**: 14-19.

Wang Y, Marshall KL, Baba Y, Gerling GJ and Lumpkin EA. 2013. Hyperelastic material properties of mouse skin under compression. *PloS one.* **8 (6)**: 1-9.

Webber LJ, Whang E and Fabo EC. 1997. The effects of UVA-I (340-400 nm), UVA-II (320-340 nm) and UVA-I+II on the photoisomerization of urocanic acid in vivo. *Photochem Photobiol.,* **66 (4)**: 484-492.

Zeigler M, Krause S, Karmiol S and Varani J. 1996. Growth factor-induced epidermal invasion of the dermis in human skin organ culture: Dermal invasion correlated with epithelial cell motility. *Invasion Metastasis.,* **16 (1)**: 3-10.

Zhang R and Zhu W. 2012. Favre-racouchot syndrome associated with eyelid papilloma: A case report. *J Biomed Res.,* **26 (6)**: 474-477.

Zuber TJ. 2002. Minimal excision technique for epidermoid (sebaceous) cysts. *Am Fam Physician.,* **65 (7)**: 1409-1420.